Nat. Hazards Earth Syst. Sci. Discuss., 2, 7367–7381, 2014
www.nat-hazards-earth-syst-sci-discuss.net/2/7367/2014/
doi:10.5194/nhessd-2-7367-2014

Natural Hazards and Earth System Sciences
Discussions
Open Access

Pre-earthquake magnetic pulses

J. Scoville[1,2,3], **J. Heraud**[4], **and F. Freund**[1,2,3]

[1]San Jose State University, Dept. of Physics, San Jose, CA 95192-0106, USA
[2]SETI Institute, Mountain View, CA 94043, USA
[3]NASA Ames Research Center, Moffett Field, CA 94035, USA
[4]Pontificia Universidad Católica del Perú, Lima, Peru

Received: 22 September 2014 – Accepted: 19 November 2014 – Published: 9 December 2014

Correspondence to: J. Scoville (atpsynthase@mail.com)

Published by Copernicus Publications on behalf of the European Geosciences Union.

Abstract

A semiconductor model of rocks is shown to describe unipolar magnetic pulses, a phenomenon that has been observed prior to earthquakes. These pulses are generated deep in the Earth's crust, in and around the Hypocentral volume, days or even weeks before Earthquakes. They are observable at the surface because their extremely long wavelength allows them to pass through kilometers of rock. Interestingly, the source of these pulses may be triangulated to pinpoint locations where stresses are building deep within the crust. We couple a semiconductor drift-diffusion model to a magnetic field in order to describe the electromagnetic effects associated with electrical currents flowing within rocks. The resulting system of equations is solved numerically and it is seen that a volume of rock may act as a diode that produces transient currents when it switches bias. These unidirectional currents are expected to produce transient unipolar magnetic pulses similar in form, amplitude, and duration to those observed before earthquakes, and this suggests that the pulses could be the result of geophysical semiconductor processes.

1 Introduction

Rocks, especially igneous rocks, behave as semiconductors under certain conditions (Freund, 2002, 2010; Freund et al., 2006; King and Freund, 1984). Although the magnetic fields produced by small semiconductors are often negligible, semiconductors on geophysical scales may produce significant magnetic fields. This is of particular interest since these fields can be observed at the Earth's surface and they seem to indicate that rock is being stressed deep in the crust.

NHESSD
2, 7367–7381, 2014

Ultra-low[1] frequency (ULF) electromagnetic emissions have been observed prior to earthquakes (Bleier et al., 2009), possibly resulting from electric currents flowing deep in the crust (Bortnik et al., 2010). Increased levels of magnetic fluctuations have been repeatedly observed prior to earthquakes since at least 1964 (Moore, 1964), but these transient phenomena are not yet fully understood and their applicability as earthquake precursors remains controversial within the geophysical community. For example, one of the most frequently cited magnetic anomalies preceded the Loma Prieta earthquake (Fraser-Smith et al., 1990). Some authors dismiss this as normal geomagnetic activity enhanced by operator or amplifier malfunction (Campbell, 2009; Thomas et al., 2009a), while counterarguments (Fraser-Smith et al., 2011) point out that continuous calibration tests should preclude this as a possiblity, that the precursor lacks the diurnal behavior of typical geomagnetic activity, and that amplifier malfunction would not preferentially amplify low-frequency signals.

Observed pre-earthquake electromagnetic waves typically have frequencies between 0.01 and 20 Hz, possibly owing to the fact that only low-frequency components may traverse tens of kilometers through the rock column. The study of such magnetic anomalies is complicated by the fact that large, unexplained variations in the magnetic field are deliberately removed from USGS data products (Thomas et al., 2009b) under the presumption that they are manmade.

During the weeks leading up to the $M = 5.4$ Alum Rock earthquake of 30 October 2007, a magnetometer located about 2 km from the epicenter recorded unusual non-alternating magnetic pulses, reaching amplitudes up to 30 nT (Bortnik et al., 2010). The incidence of these pulses increased as the day of the earthquake approached. A pair of magnetometer stations in Peru recently recorded similar unipolar pulses prior to several medium-sized earthquakes, and triangulating the source of these pulses revealed the location of subsequent earthquake epicenters (Heraud et al., 2013).

[1] In this context, "ultra-low" refers to electromagnetic waves having frequencies from millihertz to a few Hertz, in contrast to the International Telecommunications Union (ITU) definition of ultra-low, which would correspond to waves having frequencies of 300 Hz–3 kHz.

NHESSD
2, 7367–7381, 2014

The unipolar magnetic pulses observed prior to earthquakes have a characteristic shape that can be seen in Fig. 2. The unipolar nature of the magnetic pulses is somewhat unusual and bears resemblance to pulses produced by lightning and other electrical breakdown phenomena. However, the duration of many pre-earthquake pulses exceeds several seconds, much longer than any lightning strike. Moreover, triangulation of such pulses near Lima, Peru revealed that strong pulses originated almost exclusively from locations within a few kilometers of future earthquake epicenters (Heraud et al., 2013).

To model the electromagnetic phenomena associated with volumes of rock, we solve a three-dimensional drift-diffusion model of a semiconductor and calculate the magnetic fields induced by its electric currents. The model is seen to describe transient low-frequency unipolar magnetic pulses.

2 Rocks as semiconductors

The conductivity of crustal rocks in fault zones has been measured by magnetotellurics (Unsworth et al., 1999) and found to be typically 0.1–1 Sm^{-1}. These rocks are thus expected to behave as semiconductors, having conductivity typically ranging from that of silicon to germanium. We will show that unipolar pulses can emerge simply from the electrical drift and random diffusion of charge carriers in a semiconducting volume of rock. There are several reasons why this is a plausible mechanism for the observed pulses. Large electrical currents are known to accompany earthquakes, occasionally so large that luminous effects known as earthquake lights (Thériault et al., 2014) become apparent. There is experimental evidence (Freund, 2002, 2010; Freund et al., 2006; King and Freund, 1984) indicating that, during stressing, electrons and holes are freed in igneous rocks and become available to populate states in the valence and conduction bands.

One proposed source of charge carriers in rock is the break-up of peroxy defects (Freund, 2002, 2010; Freund et al., 2006) as a result of the increase in tectonic

NHESSD
2, 7367–7381, 2014

stresses. The oxygen sublattice of a wide variety of silicate minerals can form peroxy defects that act as sources of electron/hole pairs (Freund, 2010), causing these minerals to exhibit semiconductivity. Once activated, highly mobile electronic charge carriers diffuse through the minerals.

Peroxy defects are point defects, typically introduced through the incorporation of H_2O into nominally anhydrous minerals that crystallize in H_2O-laden magmas or recrystallize in high-temperature H_2O-laden environments (Freund, 2010). The incorporation of H_2O into oxides and silicates leads to OH^- pairs that subsequently undergo redox conversion. The two H^+ of the OH^- pairs combine to form H_2, and the O^- ions bind to form a peroxy bond. The formation of these peroxy bonds has been extensively studied in laboratory experiments (Freund, 2010, 2002; Freund et al., 1991; Griscom, 2011) and treated by computational chemistry (Ricci et al., 2001).

When peroxy bonds are energized via stresses in the rock or by heat, they may produce electron-hole pairs. The peroxy bond breaks, forming a transient state with two unpaired electrons. This is followed by a fully dissociated state in which a hole is free to move through the crystal structure. A neighboring oxygen atom donates an electron and becomes a hole, as its valence shell becomes deficient by one electron. The donated electron becomes trapped near the broken peroxy bond (Griscom, 2011) in a new state whose energy level is slightly below the upper edge of the valence band. In terms of the valence state, the neighboring oxygen atom, which was previously in an O^{2-} state, becomes O^-. This oxygen anion in the 1- state is effectively a positive hole with an incomplete valence shell and could also be regarded as an unstable oxygen radical (Freund, 2002).

Holes are capable of propagating through the oxygen lattice, exchanging valence electrons by a phonon-assisted vacancy hopping mechanism (Shluger et al., 1992). This process effectively constitutes a diffusion of O^- holes through a lattice of O^{2-} atoms. The trapped electrons are immobile but participate through recombination and electrostatic interactions.

NHESSD
2, 7367–7381, 2014

3 Drift-diffusion semiconductor model

The drift-diffusion equations are the most frequently used model for semiconductor physics, and perform well on scales greater than about $5\,\mathrm{m}^{-7}$ (Vasileskaet al., 2008). They describe current in terms of charge carrier concentrations and an electrostatic field, and this determines the change in charge carrier concentrations via continuity of the current density. The drift-diffusion equations are:

$$\begin{aligned}
\partial_t \boldsymbol{n} &= -\boldsymbol{R}(\boldsymbol{n},\boldsymbol{p}) + \nabla\cdot(D_n\nabla\boldsymbol{n} - \mu_n\boldsymbol{n}\nabla V)\\
\partial_t \boldsymbol{p} &= -\boldsymbol{R}(\boldsymbol{n},\boldsymbol{p}) + \nabla\cdot(D_p\nabla\boldsymbol{p} + \mu_p\boldsymbol{p}\nabla\boldsymbol{V})\\
\Delta\boldsymbol{V} &= \frac{1}{\epsilon}(\boldsymbol{n}-\boldsymbol{p}-\boldsymbol{C}).
\end{aligned} \tag{1}$$

Here, $\boldsymbol{n}$, $\boldsymbol{p}$, $\boldsymbol{R}$, $\boldsymbol{V}$, and $\boldsymbol{C}$ are defined on a domain $\Omega\times(0,T)$, where Ω is a subset of a 3-dimensional space. The functions $\boldsymbol{n}$ and $\boldsymbol{p}$ are concentrations of electron and hole charges, respectively, and $\boldsymbol{C}$ is the charge of any dopant ions that are present. $\boldsymbol{R}(\boldsymbol{n},\boldsymbol{p})$ is the recombination/generation rate of electrons and holes. The third equation is Poisson's law of electrostatics whose solution describes the electric potential $\boldsymbol{V}$. ϵ is the electric permittivity. The constants μ_n and μ_p are the mobilities of electrons and holes, respectively, (not to be confused with the magnetic permeability μ or μ_0) and D_n and D_p are the corresponding diffusion coefficients. In the particular instance of the model under consideration, μ_n and D_n are approximately zero due to electrons becoming trapped in the valence band.

4 Coupling electromagnetism to drift-diffusion

Maxwell's equations describe propagation at the speed of light, which is much faster than the charge carriers diffusing in a typical semiconductor. Rather than modeling propagation on two very different time scales, we make use of a quasi-static (magneto-static) approximation (Jackson, 1999), assuming that currents do not alternate rapidly

NHESSD
2, 7367–7381, 2014

or approach the speed of light. Specifically, the Maxwell displacement current appearing in Ampere's law is assumed to be negligible: $c^{-2}\partial_t \boldsymbol{E} \approx 0$. This assumption is implicit in the drift-diffusion model due to its use of Poisson's equation for the static electrical potential.

The electric current density $\boldsymbol{J}(\boldsymbol{x}')$ acts as the source of a magnetic field. It may be expressed as the sum of a drift term, involving the electric field, and a diffusive term, involving the concentration gradient. The rate of change of the concentration then becomes a continuity equation that is a function of current density. Explicitly separating the current and continuity equations facilitates coupling to the magnetic field. In this form, the current densities are:

$$\begin{aligned} \boldsymbol{J}_n &= D_n \nabla \boldsymbol{n} + \mu_n \boldsymbol{n} \nabla \boldsymbol{V} \\ \boldsymbol{J}_p &= -D_p \nabla \boldsymbol{p} + \mu_p \boldsymbol{p} \nabla \boldsymbol{V}. \end{aligned} \tag{2}$$

The continuity equations that describe the change in electron and hole concentrations are, then:

$$\begin{aligned} \partial_t \boldsymbol{n} &= -\boldsymbol{R}(\boldsymbol{n}, \boldsymbol{p}) + \nabla \cdot \boldsymbol{J}_n \\ \partial_t \boldsymbol{p} &= -\boldsymbol{R}(\boldsymbol{n}, \boldsymbol{p}) + \nabla \cdot (-\boldsymbol{J}_p). \end{aligned} \tag{3}$$

The current densities $\boldsymbol{J}_n$ and $\boldsymbol{J}_p$ are summed to obtain the total current density $\boldsymbol{J}$ that acts as a source for the magnetic field. In a magnetostatic approximation, the solution to the magnetic field on a domain may be efficiently computed by solving a set of Poisson equations for the magnetic vector potential. In this case, however, we calculate the field at an arbitrary point in space, which could be outside the domain. We apply the Biot–Savart law to obtain the magnetic field at the point $\boldsymbol{x}$:

$$\boldsymbol{B}(\boldsymbol{x}, t) = \frac{\mu}{4\pi} \int (\boldsymbol{J}_p(\boldsymbol{x}', t) + \boldsymbol{J}_n(\boldsymbol{x}', t)) \times \frac{\boldsymbol{x} - \boldsymbol{x}'}{|\boldsymbol{x} - \boldsymbol{x}|'^3} \mathrm{d}^3 \boldsymbol{x}'. \tag{4}$$

Here, $|\boldsymbol{x} - \boldsymbol{x}'|$ is the magnitude of the vector from $\boldsymbol{x}$ to $\boldsymbol{x}'$ and μ is the magnetic permeability. The velocities of the holes are not sufficiently large for the Lorentz force to

NHESSD
2, 7367–7381, 2014

be significantly influenced by magnetic fields so we do not conisder the effect of the magnetic field on the charge carriers.

5 Numerical solution

The drift-diffusion equations are solved by expressing the partial differential equations as a system of ordinary differential equations for the time derivatives $\partial_t \boldsymbol{n}$ and $\partial_t \boldsymbol{p}$. A finite-difference approximation to this system is then integrated using a fourth-order Runge–Kutta scheme (RK4). Poisson's equation is solved separately at each timestep using successive over-relaxation (Golub and Van Loan, 1996) (SOR) with an adaptive relaxation parameter and open boundary conditions. For the other PDEs, the Dirichlet boundary conditions $\boldsymbol{n} = 0$ and $\boldsymbol{p} = 0$ are applied to the boundary of a grid of uniformly spaced points representing the x, y, and z coordinates over which functions are evaluated. All spatial partial derivatives (∂_x, ∂_y, ∂_z, ∇) of the current and continuity equations are approximated using a fourth-order central difference approximation.

At each timestep, the electric potential is determined by solving Poisson's equation, starting the SOR iteration with the electric potential from the previous timestep. Using the electric potential and the charge carrier concentrations, the components of the current vector fields $\boldsymbol{J}_n$ and $\boldsymbol{J}_p$ are evaluated. From $\boldsymbol{J}_n$ and $\boldsymbol{J}_p$, the continuity equations are integrated, yielding the concentrations of the charge carriers at the next timestep.

The magnetic field $\boldsymbol{B}$ is evaluated by applying a discretized Biot–Savart law to the currents. $\boldsymbol{B}$ is calculated at each timestep but since the result does not affect the dynamics, it may be evaluated at a single point.

6 Results

Since holes are mobile and electrons are immobile, diffusion separates the two species, creating an electric current that acts as an electromagnet. The boundary of a region of activated charge behaves, essentially, like the p-n junction of a diode. Since only

NHESSD
2, 7367–7381, 2014

holes may flow out of this volume, the initial current diffusing across the boundary is unidirectional, corresponding to forward bias in the diode. However, after a delay period during which recombination reduces the diffusive current, the diode could switch to reverse bias, whereby the *p*-*n* junction capacitance generates a reverse recovery current. In the case of a recovery current, holes flow back into the source volume, producing a magnetic pulse that is opposite in polarity to the initial magnetic field.

We use the semiconductor model to calculate an example of a unipolar magnetic pulse. The electric permittivity and magnetic permeability are estimated based on the static properties of MgO (Batllo et al., 1991) ($\epsilon \approx 16.75\epsilon_0$ and $\mu \approx \mu_0$) and a temperature of $T = 673.15\,\mathrm{K}$. Since electrons are trapped and immobile in broken peroxy bonds, μ_n and D_n are set to 0. The mobility and diffusion constant of holes were estimated based on experimental data from an experiment in which a rapid pressure impulse to the center of a gabbro tile injected holes that diffused and drifted away from their source, akin to a Haynes–Shockley experiment. The parameters used are $\mu_p = 0.063\,\mathrm{m}^2(\mathrm{Vs})^{-1}$ and $D_p = 8.5 \times 10^{-4}\,\mathrm{m}^2\,\mathrm{s}^{-1}$, roughly comparable to their values in pure undoped Silicon.

Charge generation is not explicitly considered in this calculation, and a pre-existing excess concentration of $10^{-5}\,\mathrm{C\,m}^{-3}$ of both electrons and holes is an initial condition. These dissociated charges are initially present only at grid points inside a piriform teardrop surface of the form $(z/4000)^4 - (z/4000)^3 + (x/2000)^2 + (y/1000)^2 = 0$. Their recombination rate is proportional to the product of electron and hole concentrations, $\boldsymbol{R} = 10^{22}\boldsymbol{np}$. The attenuation of the magnetic field as it passes through the Earth is not considered, nor are effects associated with the surface of the Earth.

Calculated and observed magnetic pulses are illustrated in Figs. 1 and 2. Fig. 1 shows the value of the *x* component of the magnetic field as a function of time, measured 10 km directly above the center of the simulated volume. The amplitude, frequency, and shape of the pulse are similar to pulses that have been observed before earthquakes. For comparison, Fig. 2 shows several magnetic pulses observed prior to an earthquake near Lima, Peru. These pulses were measured over a period of sev-

NHESSD
2, 7367–7381, 2014

eral days by a pair of magnetometers approximately 25 km away, and the locations of their sources were triangulated. The sources were clustered within a few kilometers of the epicenter of an earthquake that occurred two weeks after the onset of the pulses (Heraud et al., 2013). This analysis has been performed prior to several moderate earthquakes near Lima, with similar results.

7 Conclusions

When a volume of rock is stressed, excess holes and electrons are injected. The mobile holes begin to diffuse out of the source volume, while electrons are trapped within the source volume and undergo recombination with the holes that have not diffused out. The flux of holes leaving the source effectively creates a *p*-*n* diode: the source volume becomes an *n* type semiconductor and the surrounding rock becomes *p* type. A depletion region forms between the two layers of the *p*-*n* junction and the *p*-*n* double layer screens electric fields outside its immediate vicinity.

After charge injection, a diffusive current of holes flows as a result of the concentration gradient across the source boundary. This corresponds to a forward bias state of the diode, dominated by diffusion capacitance rather than junction capacitance. This current creates a transient magnetic field. As the hole concentration gradient decreases, the diffusive current and the magnetic field decay. After holes have diffused outward, creating *p* type and *n* type regions, a junction capacitance results from layers of positive and negative charge separated by a depletion region at the junction.

After a delay period, the diode may switch to a reverse bias state. In this case, electron-hole recombination consumes the holes remaining within the source volume, leaving mostly electrons inside. The junction capacitance causes a transient reverse recovery current. If the potential drop across the depletion region is sufficiently strong, reverse-bias electrical breakdown may occur as Coulomb attraction pulls holes back into the source volume.

NHESSD
2, 7367–7381, 2014

A distinctive form and the ability to pass through the earth at ultra-low frequencies make magnetic pulses a compelling tool for the observation of pre-seismic shifts in the stress level of rocks that are otherwise inaccessible due to depth. By triangulating the source of these magnetic pulses, the increased buildup of stress around future earthquake epicenters may be identified weeks in advance of seismicity.

In addition to unipolar pulses, other types of electromagnetic precursors might be predicted from the semiconductor model. Oscillatory ULF fields, for example, have been observed immediately preceding earthquake activity (Bleier et al., 2009).

The "positive hole" semiconductor theory modeled here seeks to unify a wide range of electromagnetic phenomena associated with seismic activity. The direct coupling of semiconductor drift-diffusion currents and electromagnetism produces a model consistent with observations of pre-seismic magnetic pulses. This suggests that pre-earthquake ULF activity may be the result of geophysical semiconductor processes.

Acknowledgements. The authors would like to thank Tom Bleier and Clark Dunson of QuakeFinder for many informative discussions. The authors would also like to thank Jiro Funamoto and Kim Johnson for their comments on the manuscript. This research was funded in part by NASA Earth Surface and Interior Grant NNX12AL71G (John LaBrecque).

References

Batllo, F., LeRoy, R. C., Parvin, K., Freund, F., and Freund, M. M.: Positive holes in magnesium oxide. Correlation between magnetic, electric, and dielectric anomalies, J. Appl. Phys., 69, 6031–6033, doi:10.1063/1.347807, 1991. 7375

Bleier, T., Dunson, C., Maniscalco, M., Bryant, N., Bambery, R., and Freund, F.: Investigation of ULF magnetic pulsations, air conductivity changes, and infra red signatures associated with the 30 October Alum Rock M5.4 earthquake, Nat. Hazards Earth Syst. Sci., 9, 585–603, doi:10.5194/nhess-9-585-2009, 2009. 7369, 7377

Bortnik, J., Bleier, T. E., Dunson, C., and Freund, F.: Estimating the seismotelluric current required for observable electromagnetic ground signals, Ann. Geophys., 28, 1615–1624, doi:10.5194/angeo-28-1615-2010, 2010. 7369

NHESSD

2, 7367–7381, 2014

Campbell, W. H.: Natural magnetic disturbance fields, not precursors, preceding the Loma Prieta earthquake, J. Geophys. Res., 114, A05307, doi:10.1029/2008JA013932, 2009. 7369
Fraser-Smith, A., Bernardi, A., McGill, P., Helliwell, R., and Villard Jr., O.: Low-frequency magnetic field measurements near the epicenter of the Ms 7.1 Loma Prieta earthquake, Geophys. Res. Lett., 17, 1465–1468, 1990. 7369
Fraser-Smith, A., McGill, P., and Bernardi, A.: Comment on "Natural magnetic disturbance fields, not precursors, preceding the Loma Prieta earthquake" by Wallace H. Campbell, J. Geophys. Res., 116, 1–9, 2011. 7369
Freund, F.: Charge generation and propagation in ingneous rocks, J. Geodyn., 33, 543–570, 2002. 7368, 7370, 7371
Freund, F.: Toward a unified solid state theory for pre-earthquake signals, Acta Geophys., 58, 719–766, 2010. 7368, 7370, 7371
Freund, F., Masuda, M. M., and Freund, M. M.: Highly mobile oxygen hole-type charge carriers in fused silica, J. Mater. Res., 6, 1619–1622, 1991. 7371
Freund, F., Takeuchi, A., and Lau, B.: Electric currents streaming out of stressed igneous rocks – a step towards understanding pre-earthquake low frequency EM emissions, Phys. Chem. Earth, 31, 389–396, 2006. 7368, 7370
Golub, G. and Van Loan, C.: Matrix Computations, 3rd Edn., Johns Hopkins University Press, Baltimore, 1996. 7374
Griscom, D.: Trapped-electron centers in silica, J. Non-Cryst. Solids, 357, 1945–1962, 2011. 7371
Heraud, J., Centa, V. A., Bleier, T., and Dunson, C.: Determining future epicenters by triangulation of magnetometer pulses in Peru, in: AGU Fall Meeting, NH014, American Geophyiscal Union, Washington, D.C., 2013. 7369, 7370, 7376
Jackson, J.: Classical Electrodynamics, 3rd Edn., John Wiley and Sons, New York, 1999. 7372
King, B. and Freund, F.: Surface charges and subsurface space-charge distribution in magnesium oxides containing dissolved traces of water, Phys. Rev. B, 29, 5814–5824, 1984. 7368, 7370
Moore, G.: Magnetic disturbances preceding the 1964 Alaska earthquake, Nature, 203, 508–509, 1964. 7369
Ricci, D., Pacchioni, G., Szymanski, M., Shluger, A., and Stoneham, A.: Modeling disorder in amorphous silica with embedded clusters: the peroxy bridge defect center, Phys. Rev. B, 64, 224104, doi:10.1103/PhysRevB.64.224104, 2001. 7371

NHESSD
2, 7367–7381, 2014

Shluger, A., Heifets, E., Gale, J., and Catlow, C.: Theoretical simulation of localized holes in MgO, J. Phys.-Condens. Mat., 4, 5711–5722, 1992. 7371
Thériault, R., St-Laurent, F., Freund, F., and Derr, J.: Prevalence of earthquake lights associated with rift environments, Seismol. Res. Lett., 85, 159–178, 2014. 7370
Thomas, J. N., Love, J. J., and Johnston, M.: On the reported magnetic precursor of the 1989 Loma Prieta earthquakes, Phys. Earth Planet. In., 173, 207–215, 2009a. 7369
Thomas, J. N., Love, J. J., and Johnston, M.: On the reported magnetic precursor of the 1993 Guam earthquake, Geophys. Res. Lett., 36, L16301, doi:10.1029/2009GL039020, 2009b. 7369
Unsworth, M., Egbert, G., and Booker, J.: High-resolution electromagnetic imaging of the San Andreas fault in Central California, J. Geophys. Res., 104, 1131–1150, 1999. 7370
Vasileska, D., Mamaluy, D., Khan, H., Raleva, K., and Goodnick, S.: Semiconductor device modeling, J. Comput. Theor. Nanos., 5, 999–1030, 2008. 7372

NHESSD
2, 7367–7381, 2014

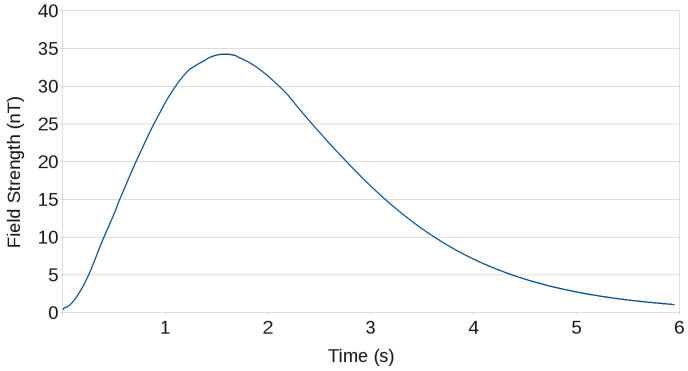

Figure 1. A calculated transient magnetic pulse, 10 km from the current source.

NHESSD
2, 7367–7381, 2014

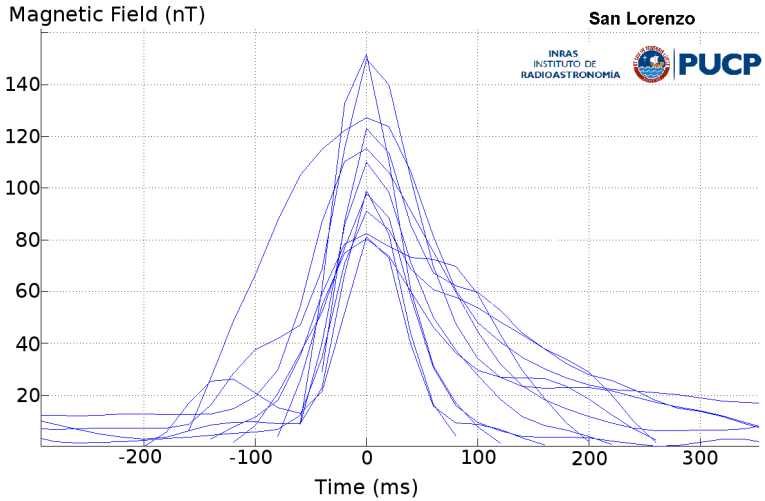

Figure 2. Magnetic pulses observed prior to an earthquake in Lima, Peru, approximately 25 km from the epicenter.

NHESSD
2, 7367–7381, 2014